

PalArch's Journal of Archaeology of Egypt / Egyptology

INVESTIGATING THE CLIMATE CHANGE TREND AND THE URBAN HEAT ISLAND OF TEHRAN DISTRICT 1 USING THE REMOTE SENSING TECHNOLOGY AND GIS

Nikoo Razavi

E.mail: nikoo.razavi65@gmail.com

Nikoo Razavi. Investigating The Climate Change Trend And The Urban Heat Island Of Tehran District 1 Using The Remote Sensing Technology And Gis -- Palarch's Journal Of Archaeology Of Egypt/Egyptology 19(2), 69-88. ISSN 1567-214x

Keywords: Urban Heat Island-GIS-Remote Sensing Technology

ABSTRACT

The rise in the earth's temperature and the formation of heat islands in metropolitan areas have turned into one of the environmental challenges resulting from the unplanned growth of these cities. These urban issues more than ever affect metropolitan areas of Iran, such as Tehran. Environmental shortages and the resulting pollution are specific instances of such problems. Global warming and the formation of heat islands in the 22 districts of Tehran are other examples of these problems that have led to recent environmental issues. Satellite images are increasingly used in urban environmental studies as they provide an integrated view and reduce the time and costs of studies. This study aims to investigate the reasons for temperature variations and the formation of a heat island in District one of Tehran following the development of this area during the past decades. Landsat TM, ETM, and OLI imagery of the years 1984 to 2020, thermal remote sensing techniques, and the GIS are used to analyze the data, and the correlation between the data was obtained via the SPSS software. The results revealed that the earth's surface temperature in district one of Tehran has increased during the past thirty-eight years. During this period, the land use in Tehran district one has changed considerably. The urban land use has increased from 16 percent in 1984 to 35 percent in 2020, and the vegetation has decreased from 32 percent to 14 percent.

Considering these findings, it is clear that the trend of temperature rise in district one of Tehran has become an environmental issue, and land-use variations such as reduced vegetation and accelerated urbanization are the factors affecting this issue.

INTRODUCTION

Urbanization is accelerating throughout the world in such a way that in 2015, 55.3% of the world's population lived in cities; however, this percentage might

rise to 68.4 by 2050 (United Nations Department of Economic and Social Affairs, 2019). Rapid urbanization leads to variations in the climate system and an increase in the production of greenhouse gases (Hattab et al, 2018), threatens biodiversity, and affects ecological productivity by disturbing the energy balance (Litardoa et al., 2020) and destroying the carbon reservoirs (Wang et al., 2021). Urbanization also leads to a significant reduction in vegetation, variations in luminance, heat, humidity, urban surface roughness, urban dispersion (LongLia et al., 2020), continuous increase in artificial surfaces such as roads and buildings, changes in radiant flux and climate, increased urban heat, and formation of urban hot spots (Tepanosyan et al., 2021). The development of this phenomenon causes the formation of urban heat islands (Shaima et al., 2021). Urban heat island is a state occurring in metropolitan areas when urban areas have higher temperatures than rural areas (Astudillo et al., 2021), and natural surfaces of the land are replaced with the buildings, roads, and other asphalted areas (Helen et al., 2021) (Kabano et al., 2020) as a result of changes in the land surface by man (Astudillo & AlKafy, 2021). This temperature increase begins from 2 degrees and can increase even more (Harun et al., 2020). Urban heat island is the main factor impacting urban climate, urban vegetation, air pollution (Li et al., 2020), human and environmental health, including vulnerable groups of the society (Wang et al., 2021), public health (Sekertekin et al., 2020) (Vasenev et al., 2021), and increased mortality rate (Koopmans et al., 2020). Land surface temperature (LST) is a key parameter of the land surface, which is applied in various scientific fields such as meteorology, hydrology, agriculture, public health, and environmental science (Wei et al., 2021). It is also a principal cause of climate change at the global level, radiant fluence between the earth's surface and the atmosphere, and the hydrologic cycle. Therefore, it is studied extensively in environmental research (XinYe et al., 2021). LST is a crucial element that controls physical, chemical, and biological processes connecting the earth and the atmosphere and considerably influences the vegetation, soil, and water (Yuan Chi et al., 2021). Remote sensing is the main source of estimating the amount of solar energy and LST mapping in case of scarcity of meteorological stations, especially in oceans, and arid and semi-arid regions of the earth (Yuan Chi et al., 2021). The spatial resolution of the sensors and the algorithms used to calculate sunshine variables, vegetation index, and land surface temperature are all elements measured by the GIS remote sensing data (Hiba et al., 2021).

Remote sensing (RS) techniques are suitable methods for obtaining experimental data directly and are effective means for environmental enhancement, managing, and supervising urban dynamics. The Geographic Information System (GIS) is a method for spatial analysis, modeling, and mapping. Many researchers have combined RS with GIS (Liu et al., 2021). Remote sensing satellites provide a simple method to study heat differences between urban and rural areas and estimate land surface temperature (LST) and urban heat islands (Ahmed, 2018). Developing thermal remote sensing is an appropriate solution for deficiency in the regular survey of the urban heat islands. Such techniques can effectively and quantitatively control the distribution characteristics of urban heat islands and periodic dynamic variations of urban heat islands (Wanga et al., 2019). Today, a new generation of thermal remote sensory devices such as the Moderate Resolution Imaging

Spectroradiometer (MODIS), the Advanced Very High-Resolution Radiometer (AVHRR), ASTER, and Landsat are free and have archives of records dating back to the 1970s (Gadrani et al., 2018).

The capital of Iran has experienced rapid urban growth since the 1990s. Tehran with a population of approximately 12 million people is the most populous city in Iran and a central hub of production, residence, commerce, distribution, and transportation in Iran (Mousavi et al., 2010). The accelerated urban growth of Tehran and the lack of proper planning have had significant impacts on its heat environment. Recent studies show that compared to Varamin's station, the minimum temperature of Tehran has increased, which indicates the release of more thermal energy in Tehran compared to its suburban areas (Akbari et al., 2010). Research on the heat island of Tehran reveals that its effects have become more evident, and its spatial and temporal specifications have changed along with the growth of metropolitan Tehran. Therefore, studying the spatial structure of the land surface temperature, the effects of the heat island of Tehran, and how to obtain the temperature of hot and polluted areas have become more important (Sadeghinia et al., 2013). Tehran District One is a significant area that has experienced substantial growth in recent decades. The trend of temperature rise is more evident in this district due to its geometrical shape and mountains. A review of the literature reveals that the term 'heat island' was first introduced by Luke Howard in 1833 (Gallo et al., 1993). Numerous researches in big, industrial cities of the world have followed, concluding that urbanization has made considerable changes in meteorologic parameters and land surface features, which has consequently caused significant changes in the local weather and climate conditions (Weng et al., 2007). According to several studies, heat island affects the temperature more than other metrological quantities. It is also stated that a gentle breeze and an anticyclone in a clear sky could prepare the ground for the formation of a reasonably intense heat island (Akbari et al., 2009; Amiri et al., 2009; Mousavi et al., 2010; Oke, 1973, 1982). A study conducted from 1931 to 1960 in London investigated the annual temperature variations. The mean annual temperature of this city was reported to be 11°C, the suburbs' temperature was three °C, and the temperature of the surrounding rural area was six °C. This temperature difference proved the occurrence of a heat island in this city (Barry and Chorley, 1987). The early studies that attempted to investigate the urban thermal perspective used thermal infrared data and the data obtained from the NOAA AVHRR sensor (Gallo et al., 1993). The spatial resolution of the thermal band for all of these studies was 1.1 km, which is only suitable for drawing small-scale maps of the city's temperature. The data obtained from Landsat ASTER, TM, and ETM thermal infrared data with spatial resolutions of 90, 60, and 120 meters respectively, made it possible to measure the land surface temperature and more precisely study the urban heat islands (Rizwan et al., 2008, p. 23). Of the studies conducted in recent years, those carried out using multispectral thermal imagery are more significant because of the possibility of discovering spatial-temporal variations of the heat islands. A substantial number of studies have applied classic statistical methods to identify spatial-temporal variations of the heat islands (Rajeshwari et al., 2014). In another study done in Beijing, China, the temperatures of land surface radiation were extracted from a TM image of the Landsat satellite, and the formation of a heat island in this city was confirmed (Lam et al., 1990). As a result,

considering the problem being studied in this study, i.e., the increase in the temperature of district one of Tehran and the formation of a heat island in this district, investigating the factors behind this problem seems necessary. Adopting a spatial, environmental perspective can resolve the problem stated in this study. Therefore, the present study explores the environmental issue of District one of Tehran and the reasons for the formation of a heat island in this city using appropriate, state-of-the-art technologies such as remote sensing (thermal remote sensing) to have an overall, spatial view of the city (the area under study: district one of Tehran), and the GIS to draw different types of maps, and model and integrate the layers. This research aims to study the city's temperature and its elements in district one of Tehran by remote sensing technology, Landsat imagery, and thermal bands from 1984 to 2020. Furthermore, the elements and parameters that affect the temperature rise are added to the land surface temperature, land use, vegetation, altitude variations, and the geometrical shape of district one of Tehran.

MATERIALS AND METHOD

The Location of the Area under Study

Tehran is the biggest and the most important city in Iran, and one of the largest cities in the world. The largeness of this capital city and its special political, economic, cultural, and geographical status, as well as the concentration of information in it compared to other parts of the country, has made many people come to this city for work, education, medical treatment, trade, and recreation and gradually settle there. This metropolitan area with its overwhelming needs and issues is directed by nearly 24 governmental or public organizations. Tehran municipality is the main body responsible for dealing with the city's issues, promoting civil participation, and citizens' satisfaction. Figure 1 shows that the metropolitan Tehran includes 22 districts. District one is located in the far northeast and the northernmost part of Tehran with latitudes of 534272.5 eastern, 5466705.5 westerns, and longitudes of 3964923.5 northern and 3964923.5 southern. This district borders Alborz Mountain to the north, Evin area to the west, Parkway and Ayatollah Sadr highways to the south, and Lavasanat to the east. Tehran District One Municipality is regarded as part of Shemiranat County. This area is also called "Shemiran". Shemiranat consists of 10 zones and 26 neighborhoods occupying approximately 3604.8944 hectares, and the population of this district in the 2016 population Census of Iran is 487,508 people (166,881 households) including 238,693 men and 248,815 women. This district has a semirural texture that can be named a 'garden city' in urban design. Shemiran is located in the foothills of the southern Alborz Mountains and has a semi-mountainous peculiar structure that is a combination of modern and traditional urban development. It is an old, significant site with favorable climate features that provides ample opportunities for construction work.

Niavaran Cultural Center, Jamaran Art Gallery, and Melal Cultural Center are this district's most notable cultural centers. Saadabad Historical Complex, Mellat Museum, Niavaran Palace, Imamzadeh Saleh, and Zahir-od-Dowleh Cemetery in Tajrish are also located in this district. Darband, Darakeh, Tochal,

Kolakchal, Evin Darakeh, Jamshidiyeh Park, and Qeytarieh are this district's recreational sites and tourist attractions. Figure 2 depicts the situation of District one of Tehran and its subdivisions.

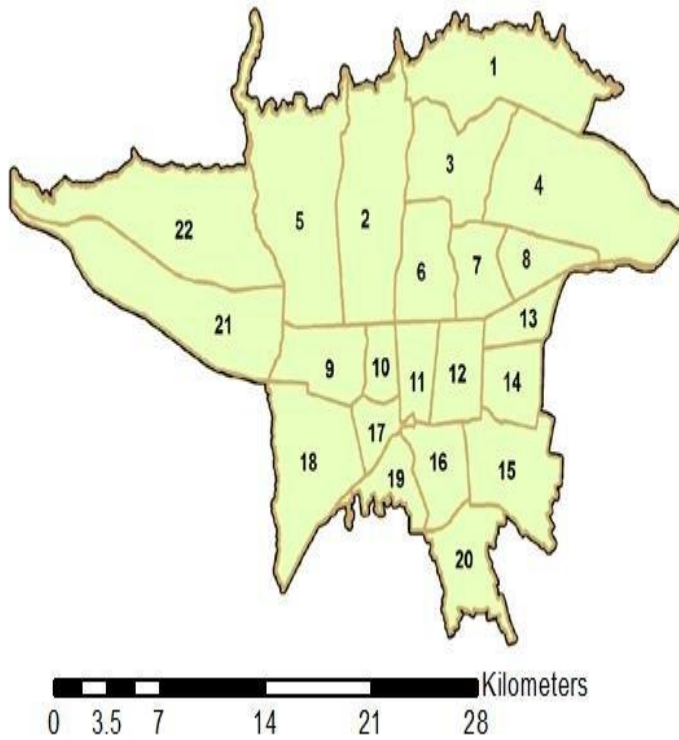


Figure 1. The geographical location of the 22 districts of Tehran

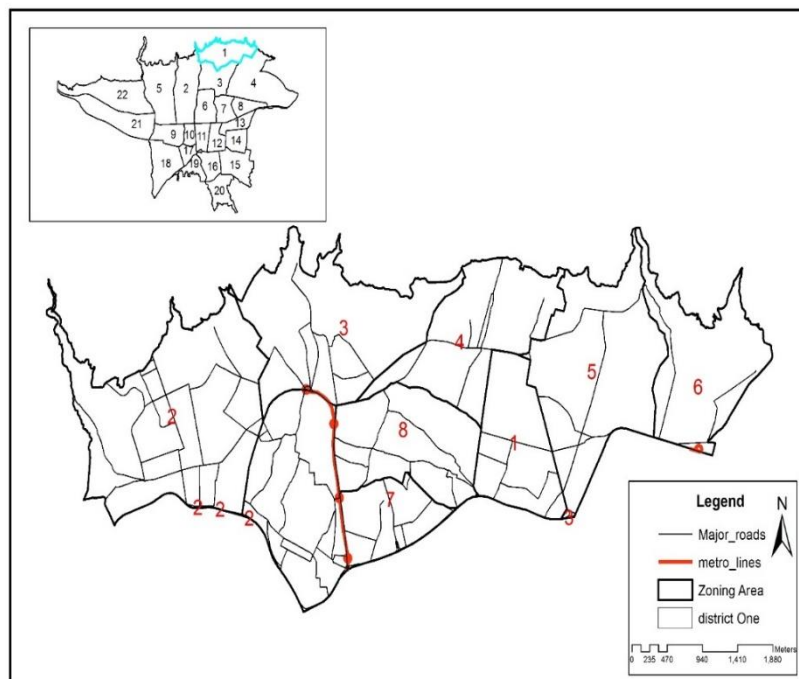


Figure 2. The geographical location of district 1 of Tehran

RESEARCH METHODOLOGY

This study is applied and descriptive-analytical. It utilizes Landsat satellite imagery for environmental and spatial analysis of district one of Tehran. TM, ETM, and OLI Landsat imagery of the years 1984, 1994, 2004, 2014, and 2020 are obtained from the USGS and NASA websites. This study also uses thermal remote sensing techniques (including 10 Landsat images) effectively combined with the GIS. The study investigates the factors affecting the rise in the land surface temperature and the formation of a heat island in district one of Tehran while considering its specific topographical conditions. An increase in the land surface temperature is one of the critical factors examined using thermal remote sensing in summer and winter. The vegetation from 1984 to 2020 is another factor studied using the Normalized Difference Vegetation Index. The three-dimensional shape of the district and its altitude which influence its climate are investigated as well. Land use is another factor that refers to the invariant, recurring features of the land surface that are separable from other features with a distinct border. Land cover map data are the basis for studying the land, which should be extracted from the raw data of remote sensing and classified before entering them into the Geographical Information System. Classification of satellite imagery is an essential part of interpreting the satellite data. Therefore, this study analyzes and classifies the images obtained from 1984 to 2020 to explore the land-use changes in district one of Tehran. The raw remote sensing data from the land surface obtained by various instruments have some errors and deficiencies that should be eliminated before using satellite images.

In addition, the present study has deployed the ARC GIS 10.5 software to provide output, ERDAS IMAGINE, ENVI 5.2, and IDRISI software packages to process and analyze Landsat images, and ultimately, determine land use, draw thermal maps, and classify them.

Components and Parameters Affecting the Land Surface Temperature in District One

Land Use

It is an influential factor in increasing the temperature of District one of Tehran because, similar to other districts of Tehran, this district has experienced several spatial variations during the past years, leading to a significant influence on the city's temperature rise in different periods.

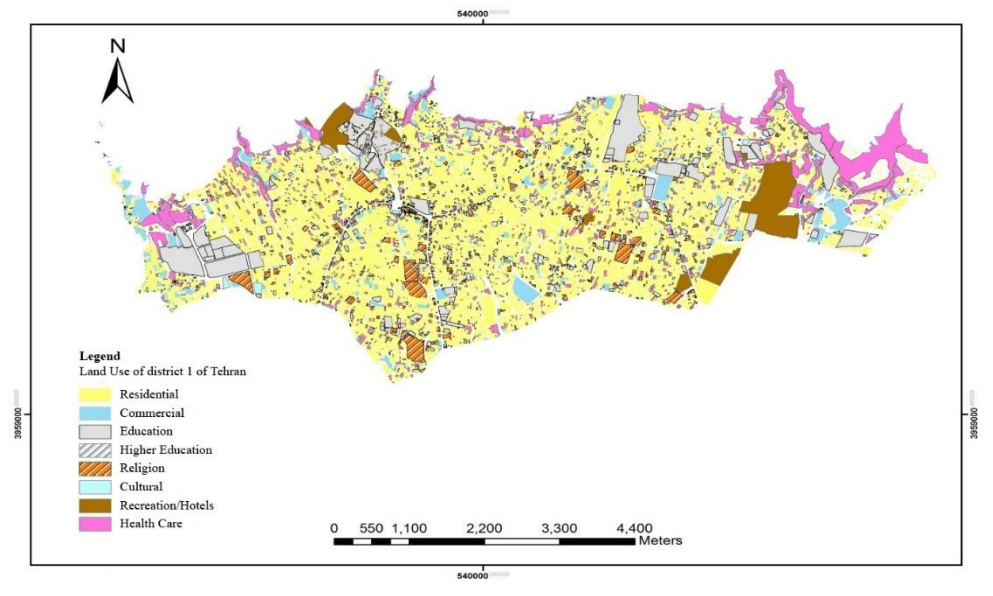


Figure 3. land use map of district one of 3Tehran separately for each use

In addition to land use, other influential factors in increasing the temperature of District one of Tehran are population growth, its dynamism, and spatial distribution, which can be observed in recent years. Population control is a significant aspect of urban management and planning, and demographic variations of many nationwide and local plans should be based on a deep understanding of the city. In case of failure to manage the issues occurring in the city based on this understanding, serious problems such as increased energy consumption and the formation of a heat island in the city may arise. Figure 4 shows the trend of partial population density of District one of Tehran. As can be seen, most density is observed in the city center, where most of the workload is done.

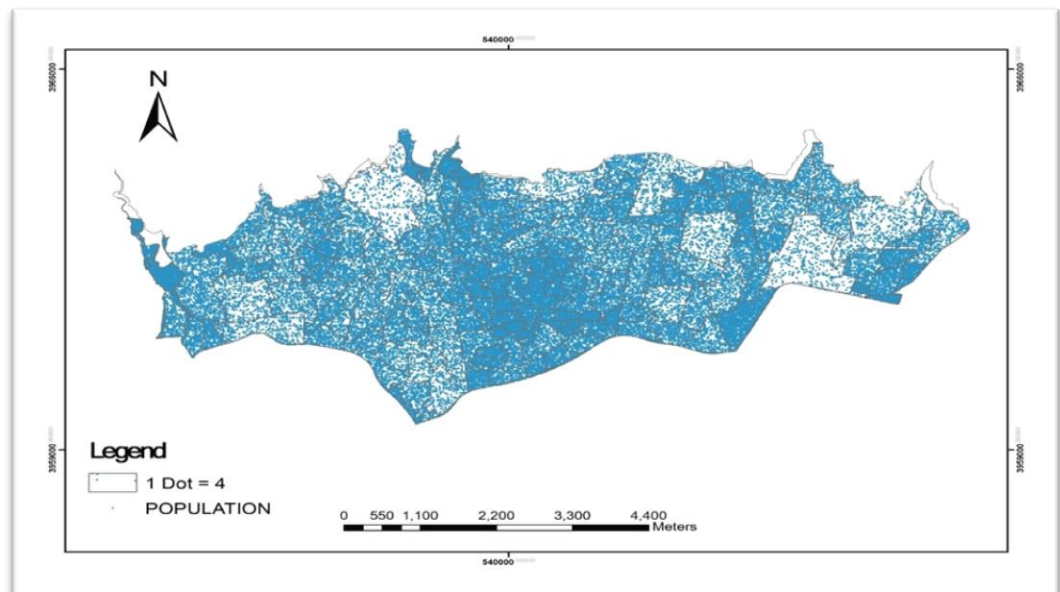


Figure 4. Map of the relative density of District one of Tehran

To study these variations, remote sensing technology, which identifies and separates land phenomena and categorizes them into distinct classes, and Landsat satellite imagery for 1984 to 2020 is used. Band combinations for Landsat images are used to acquire a user map before classification. The present research has utilized the band combination 4-3-2 for the TM-ETM-OLI sensors in which band 4 is infrared, indicating the highest reflection of vegetation in this band. Figure 5 shows the band combinations used to prepare the land use map for District one from 1984 through 2020. As can be seen, the area under study has been classified into five groups: greenery and vegetation colored green, urban land use colored pink, arid lands colored white, low-quality lands or mountains colored purple, and roads colored black.

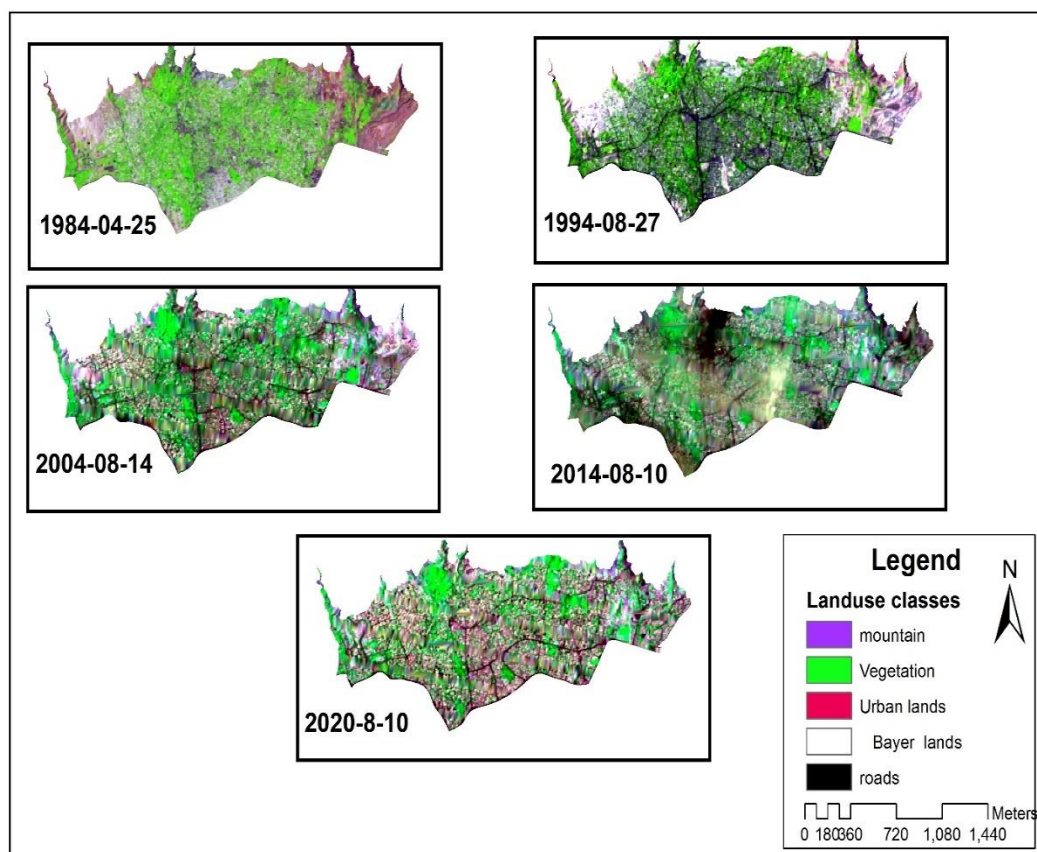


Figure 5. satellite map of land use, District one of Tehran from 1984 through 2020

After colors combination, which is also called ‘visual interpretation,’ to classify the images of the area under study, digital interpretation was applied. Many districts were first selected as samples or classes. They were categorized using the maximum estimation algorithm, considered the most precise and widely-used classification method. Following classification, classification accuracy is a criterion for valuing classification. The general accuracy of classification is calculated from (1).

$$\text{General Accuracy} = \frac{\text{Total pixels classified accurately}}{\text{Total image pixels}} \quad (1)$$

Also, the obtained accuracy, a criterion indicating the number of accurate classifications of the pixels in one category compared to the real-life pixels of the same category (Makhdoom, 2004), is described in (2).

Category x producing accuracy= Total category x accurately classified pixels/Real-life intended pixels (2)

Furthermore, the user accuracy denotes the possibility of the actual belonging of one pixel in the classified map to the same category. User accuracy is awareness of the level of confidence in the produced map, which is obtained from (3).

Accuracy of category x land use= Total category x accurately classified pixels/Category x pixels in the map (3)

Finally, Cohen's kappa coefficient (k) shows the agreement between the classification result and the real-life data. This coefficient ranges from 0-to 1, in which 1 indicates complete agreement of the classified map with the real-life phenomenon (Makhdoom, 2004). The definition of k is:

$$K = \theta_2 - \theta_1 / \theta_2 - 1 \quad (4)$$

Where θ_1 =general accuracy

θ_2 = random agreement which is calculated as follows:

$$\theta_2 = \sum I X_i + I_{x+i} / N$$

There are several methods and models for classification using remote sensing. The present research has used the maximum probability estimation algorithm due to its high accuracy of classification and reliability.

Land Surface Temperature

LST is the most crucial factor affecting temperature rise in District one of Tehran. As noted earlier, it is obtained using thermal bands of the Landsat satellite for TM-ETM-OLI sensors. To prepare a thermal map of the city's surface and obtain accurate data, the images should first be processed. The process is called 'image preprocessing' or 'image correction.' *Radiometric* is a necessary correction made on the image pixels. Part of radiometric correction is done on spectral correction images. Spectral correction takes place on digital numbers (DN) or pixels, as when an image is taken, it has digital numbers containing the data of the land surface phenomena. However, the primary data are raw (uncorrected), incapable of displaying land surface parameters such as temperature, humidity, and vegetation. For this purpose, to apply the land surface parameters to satellite images, we should correct the digital numbers. The number of pixels comprising each image should be converted into radiance and reflection, called a spectral correction. There are several models and techniques to convert the pixels of satellite images into radiance and reflection. To convert the raw image numbers to radiance for TM and ETM Landsat imagery, (5) is used (Chander et al., 2009).

$$(5) L\lambda = \left(\frac{LMAX-LMIN}{Qcalmax-Qcalmin} \right) (Qcal - Qcalmin) + LMIN$$

where $L\lambda$ is the spectral radiance in the sensor, $Qcal$ is the pixel value in the intended band, $Qcalmin$ is the minimum pixel value, $Qcalmax$ is the maximum pixel value, $LMIN$ is the minimum, and $LMAX$ the maximum spectral radiance in the sensor. The reflection coefficient for the sensor Landsat TM5.ETM7 is calculated by (6):

$$(6) p\lambda = \frac{\pi \times L\lambda \times d^2}{ESUN \lambda \times \cos \theta}$$

where $p\lambda$ is the reflection coefficient, $\pi=3.1459$, $L\lambda$ is the spectral radiance in the sensor, d is the earth's distance to the sun (astronomical unit), $ESUN$ is the mean sunshine, and θ is the sun angle (degree).

To calculate the spectral radiance in the OLI sensor, (7) is used:

$$(7) L\lambda = ML * Qcal + AL$$

where $L\lambda$ is radiance above the atmosphere, ML (watts/m²*srad* μ m) is multiplicative conversion rate, $Qcal$ is pixel values of 10 & 11, and AL is cumulative conversion rate.

Obtaining the Brightness Temperature

Thermal bands data can be converted from the spectral radiance in the sensor into the brightness temperature. Brightness temperature assumes the earth as a black object and includes atmospheric effects (absorption and radiation). Relationship (8) is applied to obtain the brightness temperature for Landsat sensors (Rajeshwari et al., 2014).

$$(8) T = \frac{K2}{Ln\left(\frac{K1}{L\lambda} + 1\right)}$$

T is the effective brightness temperature in the sensor in Kelvin, $K2$ is calibration coefficient 2 in Kelvin, $K1$ is calibration coefficient 1 in W (m st μ m), and $L\lambda$ is the spectral radiance in the sensor. $K1$ and $K2$ coefficients are calculated based on Table (1).

Table 1
K1 and K2 coefficients for Landsat satellite

Sensor Coefficient	Calibration Coefficient 1	Calibration Coefficient 2 (K)
L5-TM B6	607.76	1260.56
L7-ETM+B6	666.09	1282.71
L8-OLI B10	777.89	1321.08
L8-OLI B11	480.89	1201.14

To this aim, satellite images of District one of Tehran were calibrated, and the required corrections were made. The algorithms were used to prepare thermal maps and the thermal classification plan of District one of Tehran from 1984 to 2020.

Vegetation

Vegetation density is a crucial element in increasing the temperature of District one of Tehran and can be obtained using the Landsat satellite imagery and the vegetation index.

NDVI is a well-known, simple and applicable index used in vegetation study. NDVI uses a simple calculation process and has the best dynamic potential compared to other indexes. This index has the highest sensitivity to vegetation variations and is less sensitive to atmospheric effects and the soil background except where vegetation is scarce. NDVI is calculated from (9):

$$(9) \quad NDVI = \frac{NIR-RED}{NIR+RED}$$

where NIR is near-infrared reflectance and RED is red reflectance. Although theoretically, this index ranges between -1 and 1, practically, it ranges between less than one and more than -1. The values of this index for dense vegetation tend to be one, but clouds, snow, and water are indicated with negative values. The rocks and arid soil with similar spectral reactions in two bands are allotted values close to zero (Babaei et al., 2016). In this index, typical soil is considered equal to 1. The distance of the pixel above the soil indicates the vegetation. Therefore, the vegetation index NDVI was applied to Landsat images. The vegetation map of District one from 1984 through 2020 was produced in five classes: very low density=red, relatively low density=orange, medium density=yellow, relatively high density=light green, and very high density=dark green.

RESEARCH FINDINGS

Land surface temperature significantly affects the temperature rise in District one of Tehran. The thermal classification map was drawn using TM and ETM Landsat thermal images in band six and Oli in the thermals bands 10 and 11 in summer and winter from 1984 to 2020.

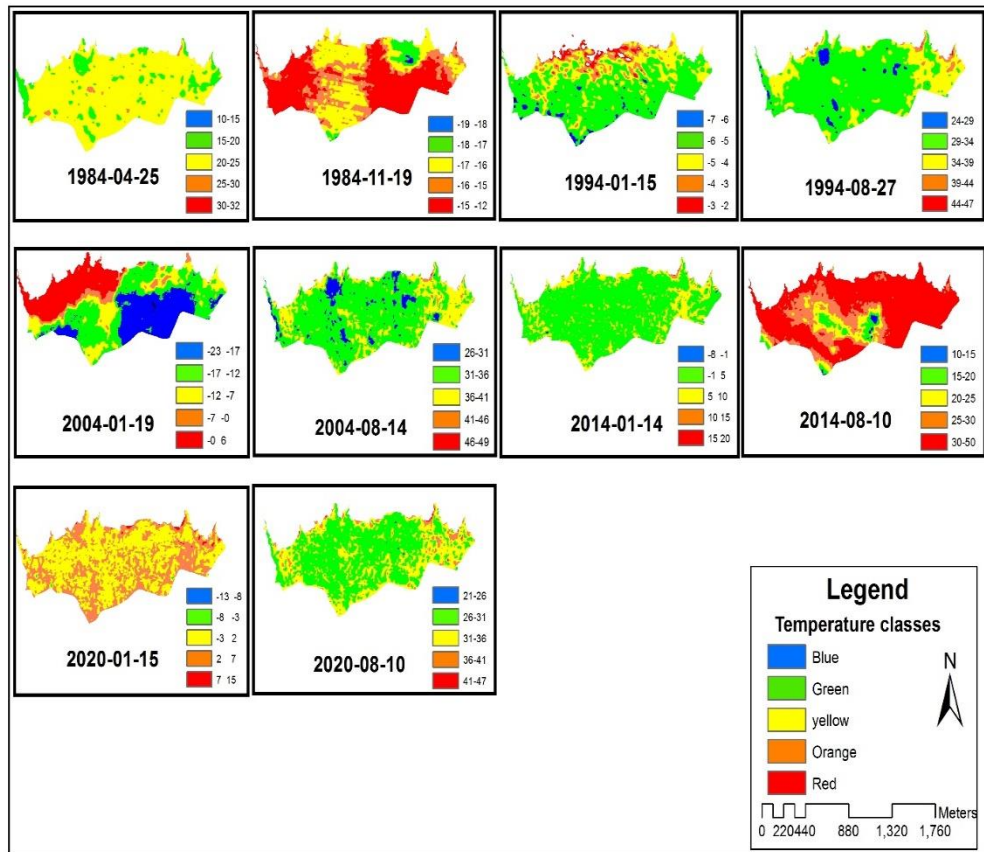


Figure 6. The land surface temperature map of District one of Tehran from 1984 to 2020

Then, the area under study was classified into five categories: blue, green, yellow, orange, and red, each indicating the related temperature in centigrade.

Table 2

Classification of the land surface temperature using Landsat thermal images

year	Categories				
	Blue	Green	Yellow	Orange	Red
- 04 – 25 1984	10 - 15	15 - 20	20 – 25	25 - 30	30 - 32
- 11 – 19 1984	-18 - -19	-17 - -18	-16 - -17	-15 - -16	-15 - -12
- 08 – 27 1994	24 - 29	29 - 34	34 - 39	39 - 44	44 – 47
- 01 – 15 1994	-06 - -07	-06 - -05	-05 - -04	-04- -03	-03 - -02
- 08 – 14 2004	26 - 31	31 - 36	36 - 41	41 - 46	46 - 49
- 01 – 19 2004	-23 - -17	-17 - -12	-12 - -07	-07 – 00	00 - -06
- 08 – 10 2014	10 - 15	15 - 20	20 - 25	25 - 30	30 – 50

- 01 - 14 2014	-08 - -01	-01 - 05	05 - 10	10 - 15	15 - 20
- 08 - 10 2020	21 - 26	26 - 31	31 - 36	36 - 41	41 - 47
- 01 - 15 2020	-13 - -08	-08 - -03	-08 - 02	02 - 07	07 - 15

As observed in Table 2, the surface temperature of District one tended to rise from 1984 to 2020, both in summer and winter. The blue category in summer in 1984 ranged between 10 to 15 °C; however, in 2020, the temperature of this category has changed to 21-26 °C. The red category indicating the highest density had values ranging between 30 to 32 °C in 1984, reaching 50 °C in 2014 and 47 °C in 2020. In winter, the temperature has increased from -18 °C to 15 °C in 2020, denoting climate change, a rise in the land surface temperature of District one of Tehran, and a heat island in this area. Land use is another influential element in land surface temperature variations in District one of Tehran. The land-use variations map for District one of Tehran was prepared using the Landsat satellite imagery, supervised classification, and the maximum probability algorithm from 1984 to 2020 in the five categories: vegetation, urban land use, arid lands, and low-quality lands, mountains, and roads.

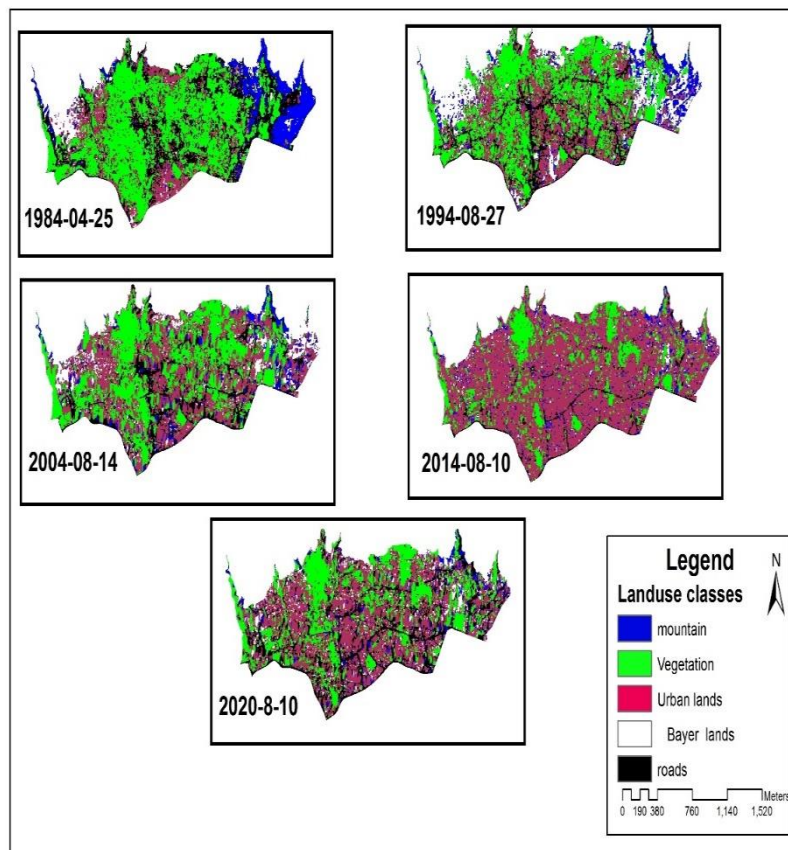


Figure 7. land use classification map of District one of Tehran from 1984 to 2020

Following the preparation of the land-use variations map, the area percentage of each land use category and the accuracy of the categories were obtained by Cohen’s kappa coefficient (k).

Table 3

The area percentage of each land use category using the Landsat imagery

Year	Land Use Area (Percentage)					Kappa Coefficient (Percentage)
	Vegetation	Urban	Arid Lands	Mountains	Roads	
1984	32.597	16.795	24.039	18.594	7.976	96
1994	26.502	26.038	15.978	18.628	12.855	97
2004	26.015	32.834	11.679	15.754	13.718	97
2014	14.155	35.745	12.497	19.271	18.331	97
2020	22.065	35.949	9.909	12.820	19.257	97

Table 3 shows that land use in District one of Tehran has experienced significant variations from 1984 to 2020. We observe an increase in urban land use from 16 percent in 1984 to 35 percent in 2020 and a decline in vegetation from 32 percent in 1984 to 14 percent in 2020. Besides, arid lands have increased from 24 percent in 1984 to 9 percent in 2020, and the roads have grown from 7 percent to 19 percent. Figure 8 depicts the trend of land use variations in District one from 1984 to 2020.

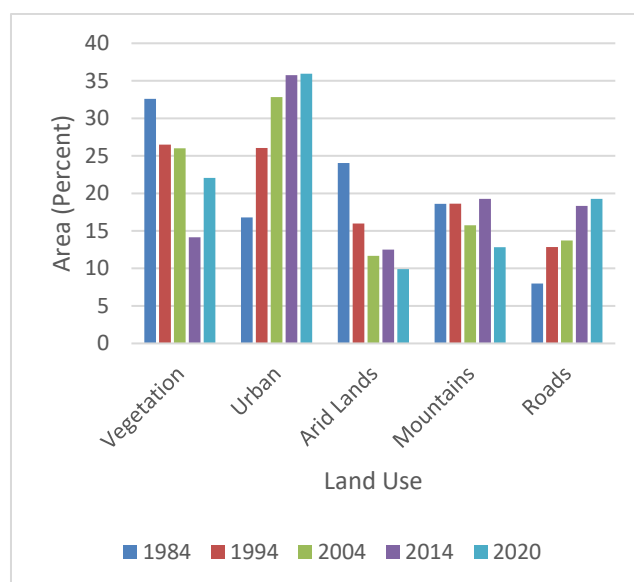


Figure 8. The trend of land use variations of District one from 1984 to 2020

Also, to explore the vegetation trend in District one of Tehran, the NDVI was applied. It was calculated for the Landsat images for 1984, 1994, 2004, 2014, and 2020. The red spots indicate areas lacking vegetation on this map, and the

green shows vegetation. Comparing the NDVI maps reveals a drop in vegetation in the area under study during the past thirty-eight years.

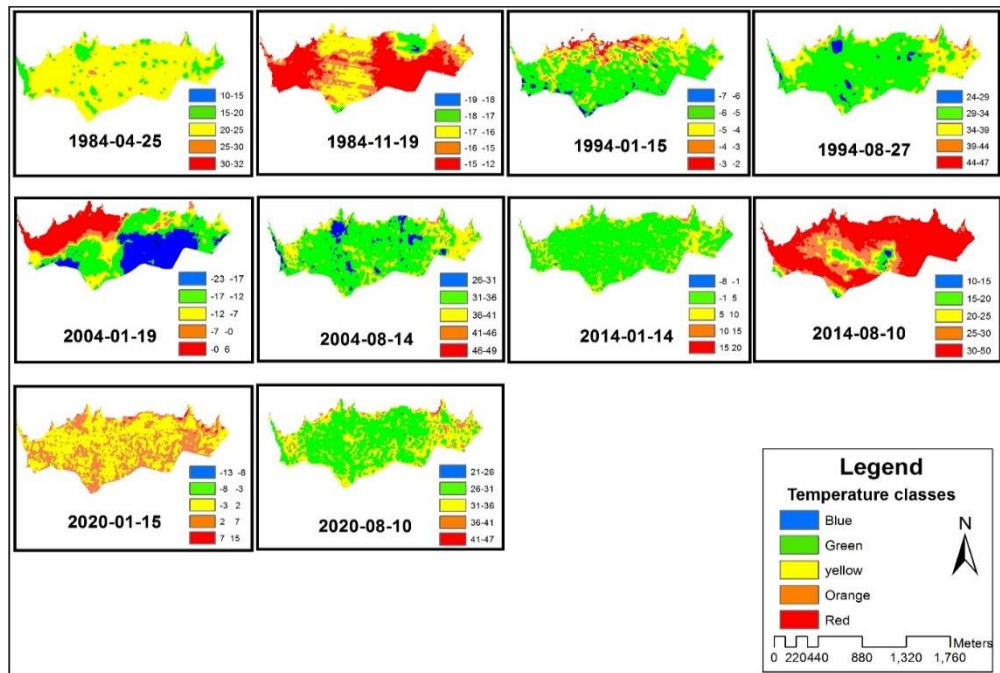


Figure 9. The vegetation index map of District one of Tehran from 1984 to 2020

Altitude Variations

Altitude variations and the geometrical three-dimensional shape of District one of Tehran are other components impacting climate and environmental changes in this district of Tehran. Most of the neighborhoods (such as Poonak, Islamic Azad University Science and Research Branch, Hesar) in this district are at higher altitudes. Figure 10 pictures the Digital Elevation Model of District one with 5-meter accuracy. Most of the neighborhoods in district one of Tehran are situated at 1400 to 1835 meters altitudes.

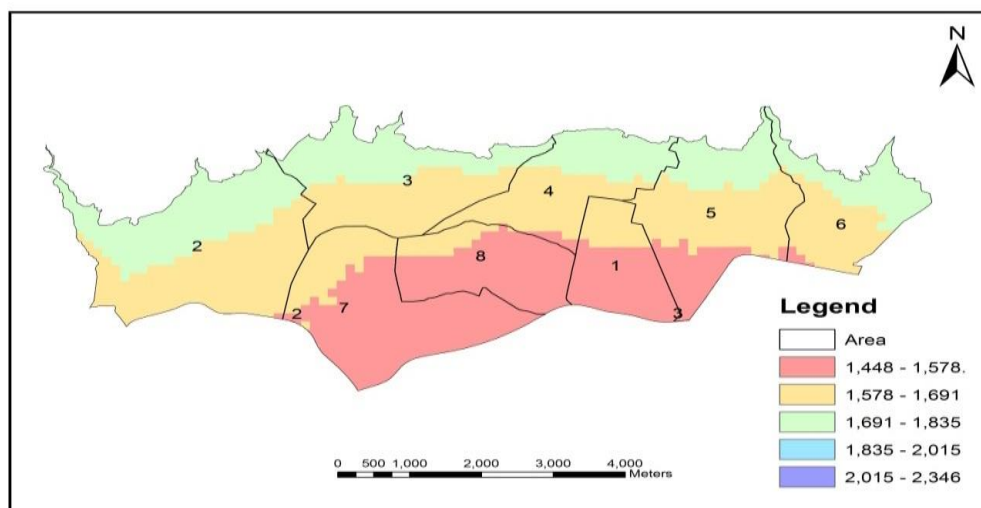


Figure 10. The Digital Elevation Model of District One of Tehran

According to Figure 11, drawn with some vertical exaggeration, mountains, low-quality lands, and the high altitude of most areas, neighborhoods, and residential areas (colored yellow) of District one of Tehran are indicated in this model. These areas have surrounded the mountains like a puddle. These mountains and low-quality lands act as a barrier blocking winds and floods from entering these areas. They are highly effective in thermal variations and lead to a rise in the temperature of this district in Tehran.

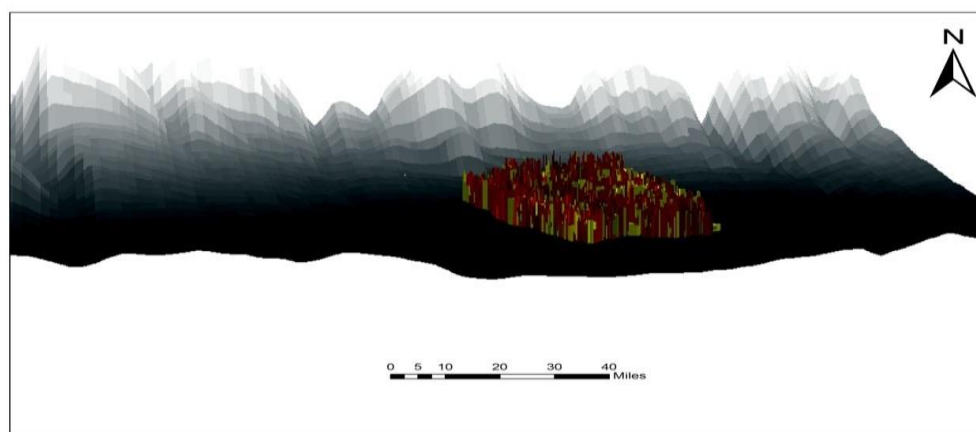


Figure 10. Exaggerated Digital Elevation Model of District One of Tehran

DISCUSSION AND CONCLUSION

The present research aims to study the trend of thermal variations in District one of Tehran, together with the elements and factors influencing them using Landsat satellite images and TM, ETM, OLI sensors, and thermal bands for 1984, 1994, 2004, 2014, 2020. This research considered the parameters: land surface temperature (LST), land use, vegetation, altitude variations, and the geometrical shapes of District one of Tehran. The trend of temperature variations in winter and summer in District one of Tehran was explored using Landsat satellite images and thermal bands; then, the land surface classification map and the vegetation density map were prepared in five categories from 1984 to 2020 (10 thermal maps). Land use map, classification, and vegetation density map were drawn using the NDVI from 1984 to 2020. In addition, this study utilized ARC GIS 10.5 to generate output; and used ERDAS IMAGINE, ENVI 5.2, and IDRISI 17 to process and analyze Landsat satellite images, determine land use, and prepare thermal maps and make the classification. The results revealed that the land surface temperature of District one of Tehran has risen in winters and summers from 1984 to 2020, as the blue category has increased from 21 to 26 °C in the year 2020.

Additionally, the red category ranged between 30-32 °C in 1984, while it rose to 50 °C in 2014 and 47 °C in 2020. Land use has had significant variation during this period, i.e., the urban land use has increased from 16 percent in 1984 to 35 percent in 2020, and vegetation percentage has fallen from 32 percent to 14 percent during this period. The analysis of vegetation using the NDVI also indicates a decline for the said period.

Altitude variations and the geometrical and three-dimensional shape of this district of Tehran are other factors affecting thermal variations in District one of Tehran. Most neighborhoods of this district are located in the altitudes of 1400 to 1835 meters. These high altitudes block the rainfalls and climatic elements, thus gradually leading to a rise in the temperature of this surface compared to other areas. According to these findings, the rising temperature trend in District one of Tehran continues, and land-use variations such as declining vegetation and increased urban land use exacerbate this trend. Besides vegetation destruction and increased building population growths, it causes impervious surfaces to overheat and transfer this excess heat to the environment. This population growth, along with the change in land use, results in the destruction of a significant percentage of natural surface vegetation and their replacement with buildings, roads, and other urban facilities. Also, reduced vegetation replaced with high-rise buildings causes an increase in the city's temperature since vegetation is crucial for absorbing urban pollutants, provides appropriate biodiversity, and prevents temperature rise in cities.

REFERENCES

- Ahmed, S. (2018). Assessment of urban heat islands and impact of climate change on socioeconomic over Suez Governorate using remote sensing and GIS techniques. *The Egyptian Journal of Remote Sensing and Space Sciences*, 21, 15–25.
- Akbari, H. (2000). Consideration of Temperature distribution pattern of Tehran using Landsat TM thermal data. A dissertation submitted to Tarbiatmodarres University for degree of MA of Remote sensing and GIS, department of human science.
- Al-Masaodi, H.J.O. Al-Zubaidi, H.A.M. (2021). Spatial-temporal changes of land surface temperature and land cover over Babylon Governorate, Iraq. *Materials Today: Proceedings*.
- Amiri, R. Weng, Q. Alimohammadi, A. Alavipanah, S.K. (2009). Spatial-temporal dynamics of land surface temperature in relation to fractional vegetation cover and land use/cover in the Tabriz urban area, Iran. *Remote sensing of environment*. 113(12), 2606-2617.
- Barry, R. Chorley, R.J. (1987). *Atmosphere, Weather and climate*. Routledge.
- Chi, Y. Sun, J. Sun, Y. Liu, Sh. Fu, Z. (2020). Multi-temporal characterization of land surface temperature and its relationships with normalized difference vegetation index and soil moisture content in the Yellow River Delta, China. *Global Ecology and Conservation* 23, e01092.
- El-Hadidy, Sh. (2021). The relationship between urban heat islands and geological hazards in Mokattam plateau, Cairo, Egypt. *The Egyptian Journal of Remote Sensing and Space Sciences*, 24(3), 547-557.
- El-Hattab M., Amany S.M., Lamia G.E. (2018). Monitoring and assessment of urban heat islands over the Southern region of Cairo Governorate, Egypt *The Egyptian Journal of Remote Sensing and Space Sciences* 21, 311–323.
- From: <https://www.routledge.com/Atmosphere-Weather-and-Climatology/Barry-Chorley/p/book/9780415465700>
- Gadrani, L. Lominadze, G. Tsitsagi, M. (2018). Assessment of landuse/landcover (LULC) change of Tbilisi and surrounding area using

- remote sensing (RS) and GIS. *Annals of Agrarian Science*, 16(2), 163–169
- Gupta, N. Mathew, A. Khandelwal, S. (2019). Analysis of cooling effect of water bodies on land surface temperature in nearby region: A case study of Ahmedabad and Chandigarh cities in India. *The Egyptian Journal of Remote Sensing and Space Sciences*, 22(1), 81–93.
- Harun, Z. Reda, E. Abdulrazzaq, A. Abbas, A. A. Yusup, Y. Zaki, Sh.A. (2020). Urban heat island in the modern tropical Kuala Lumpur: Comparative weight of the different parameters. *Alexandria Engineering Journal*, 59(6), 4475–4489.
- Kabano, P. Lindley, S. Harris, A. (2021). Evidence of urban heat island impacts on the vegetation growing season length in a tropical city. *Landscape and Urban Planning*, 206, 103989
- Koopmans, S. Heusinkveld, B.G. Steeneveld, G.J. (2020). A standardized Physical Equivalent Temperature urban heat map at 1-m spatial resolution to facilitate climate stress tests in the Netherlands. *Building and Environment*, 181, 106984.
- Lam N. S. N. (1990). Description and measurement of Landsat TM images using fractals, *Photogrammetric engineering and remote sensing*, 56(2), 188-195.
- Li, H. Zhou, Y. Jia, G. Zhao, K. Dong, J. (2022). Quantifying the response of surface urban heat island to urbanization using the annual temperature cycle model. *Geoscience Frontiers*, 13(1), 101141.
- Lia, L. Zhaa, Y. Zhangb, J. (2020). Spatially non-stationary effect of underlying driving factors on surface urban heat islands in global major cities. *International journal of Applied Earth Observation and Geoinformation*, 90, 102131.
- Litardoa, J. Palmec, M. Borbor-Cordovaf, M. Caizad, R. Maciasf, J. Hidalgo-Leona, R. Sorianoa, G. (2020). Urban Heat Island intensity and buildings' energy needs in Duran, Ecuador: Simulation studies and proposal of mitigation strategies, *Sustainable Cities and Society* 62, 102387
- Liu, Ch. Yang, M. Hou, Y. Zhao, Y. Xue, X. (2021). Spatiotemporal evolution of island ecological quality under different urban densities: A comparative analysis of Xiamen and Kinmen Islands, southeast China. *Ecological Indicators*, 124, 107438.
- Macintyre, H. L. Heaviside, C. Cai, X. Phalkey, R. (2021). The winter urban heat island: Impacts on cold-related mortality in a highly urbanized European region for present and future climate. *Environment International*, 154, 106530.
- Makhdoom, M. Darvishsefat, A.A. (2004). Environmental assessment and planning with "GIS". University of Tehran, Publishing and Printing Institute
- Mendez-Astudillo, J. Lau, L. Tang, Y. Moore, T. (2021). A new Global Navigation Satellite System (GNSS) based method for urban heat island intensity monitoring. *International Journal of Applied Earth Observations and Geoinformation*, 94, 102222
- Morsy, M. Aboelkhair, H. (2021). Assessment of agricultural expansion and its impact on land surface temperature in El-Beheira Governorate, Egypt.

- The Egyptian Journal of Remote Sensing and Space Science, 24(3), 721-733.
- Mousavi-Baygi, M. Ashraf, B. Miyanabady, A. (2010). The Investigation of Tehran's Heat Island by using the Surface Ozone and Temperature Data. *International Journal of Applied Environmental Sciences*, 5(2), 189–200.
- Naim, N.H. Kafy, A.A. (2021). Assessment of urban thermal field variance index and defining the relationship between land cover and surface temperature in Chattogram city: A remote sensing and statistical approach. *Environmental Challenges*, 4, 100107.
- Oke, T.R. (1973). City size and the urban heat island. *Atmospheric Environment*, 7(8), 769-779.
- Oke, T.R. (1982). The energetic basis of urban heat island. *Journal of the Royal Meteorological Society*, 108(455), 1-24.
- Rajeshwari, A. Mani, N.D. (2014). Estimation of land surface temperature of dindigul district using landsat 8 data. *International Journal of Research in Engineering and Technology*, 3, 2319-1163.
- Rizwan, A. M. Dennis, L. Y. Liu, C. (2008). A review on the generation, determination and mitigation of Urban Heat Island. *Journal of Environmental Sciences*, 20(1), 120-128
- Sadeghinia, A. Alijani, B. Ziaeiian, P. Khaledi, S.H. (2013). Application of spatial autocorrelation techniques in the analysis of the thermal island of Tehran. *Applied Research in Geographical Sciences*, 30, 67-90.
- Sekertekin, A. Zadbagher, E. (2021). Simulation of future land surface temperature distribution and evaluating surface urban heat island based on impervious surface area. *Ecological Indicators*, 122, 107230.
- Tepanosyan, G. Muradyan, V. Hovsepyan, A. Pinigin, G. Medvedev, A. Asmaryan, Sh. (2021). Studying spatial-temporal changes and relationship of land cover and surface Urban Heat Island derived through remote sensing in Yerevan, Armenia. *Building and Environment*, 187, 107390.
- United Nations Department of Economic and Social Affairs. (2019). *World Urbanization Prospects: The 2018 Revision*. From: <https://doi.org/10.18356/b9e995fe-en>.
- Vasenev, V. Varentsova, M. Konstantinov, P. Romzaykina, O. Kanareykina, I. Dvornikov, Y. Manukyana, V. (2021). Projecting urban heat island effect on the spatial-temporal variation of microbial respiration in urban soils of Moscow megalopolis. *Science of the Total Environment*, 786, 147457.
- Wang, Y. Yi, G. Zhou, X. Zhang, T. Bie, X. Li, J. Ji, B. (2021). Spatial distribution and influencing factors on urban land surface temperature of twelve megacities in China from 2000 to 2017. *Ecological Indicators*, 125, 107533
- Wang, Z. Meng, Q. Allam, M. Hu, D. Zhang, L. Menenti, M. (2021). Environmental and anthropogenic drivers of surface urban heat island intensity: A case-study in the Yangtze River Delta, China. *Ecological Indicators*, 128, 107845.
- Wanga, W. Liu, K. Tang, R. Wang, Sh. (2019). Remote sensing image-based analysis of the urban heat island effect in Shenzhen, China. *Physics and Chemistry of the Earth*, 110, 168–175

- Wei, B. Bao, Y. Yu, Sh. Yin, Sh. Zhang, Y. (2021). Analysis of land surface temperature variation based on MODIS data a case study of the agricultural pastoral ecotone of northern China. *International Journal of Applied Earth Observations and Geoinformation*, 100, 102342.
- Weng, Q. (2009). Thermal infrared remote sensing for urban climate and environmental studies: Methods, applications, and trends. *ISPRS Journal of Photogrammetry and Remote Sensing*, 64(4), 335-344.
- Ye, X. Ren, H. Liang, Y. Zhu, J. Guo, J. Nie, J. Zeng, H. Zhao, Y. Qian, Y. (2021). Cross-calibration of Chinese Gaofen-5 thermal infrared images and its improvement on land surface temperature retrieval. *International Journal of Applied Earth Observations and Geoinformation*, 101, 102357.